Effect of V, Nb, and Ta Doping on the 2223 Phase Formation and the Crystal Structure in the BiSrCaCuO System

Yanrong Li,[1] Bangchao Yang, and Xingzhao Liu

Department of Information Material and Engineering, University of Electronic Science and Technology of China, Chengdu 610054, People's Republic of China

and

Youmo Li

Changchun Institute of Applied Chemistry, Chinese Academy of Sciences, Changchun 130022, People's Republic of China

X-ray diffraction and electrical and diamagnetic analyses revealed that the 2223 phase was significantly enhanced by high-valence cation (V^{5+}, Nb^{5+}, Ta^{5+}, etc.) doping in BiSrCaCuO samples. The optimum nominal composition was $Bi_{1.6}M_{0.4}Sr_2Ca_2Cu_3O_y$ (M = high-valence cations) for all three elements. A quasi-high-valence peak of $Cu_{2p_{3/2}}$ (~534.5 eV) has been observed. A reversible reaction, $Bi^{3+} \underset{\text{annealed}}{\overset{\text{quenched}}{\rightleftharpoons}} Bi^{5+} + Bi^+$, was also encountered in the sample doped with Nb^{5+}. The effects of doping high-valence cations on the high-T_c phase formation and the crystal structure are two-fold: (1) The high-valence cation substitution for the fourfold-coordinated Cu site in the CuO_2 sheet strengthens the coupling among the $Ca–CuO_2–Ca$ layers of the 110 K phase, and (2) the cations incorporated into the Bi–O layers increase the oxygen bonding, which is beneficial for the formation of the Aurivillius-type structures and stabilizes the structure of the 2223 phase. We argue that the beneficial effect for promoting the formation of the 2223 phase might be a general property of doping with high-valence cations. © 1994 Academic Press, Inc.

1. INTRODUCTION

Since the disclosure of the BiSrCaCuO superconductor series (1), the substitution of some Bi with Pb has been the most effective way for stabilizing and promoting formation of the high-T_c 2223 phase (2). Recently, doping with Sb has also been found to promote formation of the 2223 phase (3). Here, we have systematically studied the effect of the high-valence cations V^{5+}, Nb^{5+} and Ta^{5+} on the formation of the high-T_c 2223 phase and have found that doping by any one of them significantly enhances

[1] To whom correspondence should be addressed.

formation of the 2223 phase; their role is quite similar to that of Pb for stabilizing the 2223 phase.

2. EXPERIMENTAL

Samples of nominal composition $Bi_{2-x}M_xSr_2Ca_2Cu_{3-y}M_yO_z$ (M = V, Nb, or Ta; $x = 0 \sim 1.0$; $y = 0 \sim 0.5$) were prepared from analytical reagent grade Bi_2O_3, $SrCO_3$, $CaCO_3$, CuO, V_2O_5, Nb_2O_5, and Ta_2O_5, which were preheated at 800°C for 20 hr in air, pelleted, and again heated at 800°C for 10 min, allowing the low-melting-point compound to react and to form the intermediate compound. The temperature was then raised slowly (~2°C/min) to ~860°C, where it was kept for ~40 hr. The sample was then quenched in air.

X-ray powder diffraction (XRD) was performed on D/max-IIB equipment. The resistance dependence of temperature ($R \sim T$) was measured by the standard four-probe method with In contacts. Alternating current magnetic susceptibility (ac χ) measurements were carried out by a mutual induction method with a precision of -5×10^{-6} V and ± 0.15 K. The X-ray photoemission spectrum (XPS) data for core levels of each element were collected on a VG ESCALAB MK spectrometer; the pressure during the measurements was 1×10^{-9} mbar.

3. RESULTS AND DISCUSSION

Figure 1 shows the XRD patterns of $Bi_{1.6}Nb_{0.4}Sr_2Ca_2Cu_3O_y$ under different heat-treatment conditions. $Bi_2Sr_2CuO_6$ (2201 phase) and some intermediate phases including $Sr_{0.82}NbO_3$, Ca_2CuO_3, and CuO are first formed at 780°C; they then gradually decay while the 2212 phase begins to grow in the process of flash heating at 880°C.

FIG. 1. Fired temperature dependence of the forming phase for $Bi_{1.6}Nb_{0.4}Sr_2Ca_2Cu_3O_y$.

amount of the 2223 phase begins to decrease; the optimum amount occurs at $x = 0.4$. Obviously, the 2223 phase is significantly enhanced by doping with the high-valence cation. The diffraction peaks of the 2212 and 2223 phases show a slight reduction of the lattice parameters with increasing [Nb]. This is perhaps caused by the high-valence cation entering into the lattice, which enhances bonding between the layers (4). Moreover, the width of the diffraction peaks broadens and becomes more diffuse with Nb doping; this effect may be due to lattice distortion. At the same time, with increasing doping the peaks of CuO and the peaks located at $2\theta \sim 31°$ of the $Sr_{0.82}NbO_3$ phase increase. The rise of the amount of CuO with Nb doping indicates that Cu in the lattice is replaced by Nb. The amount of the 2223 phase also increases with increasing Nb substitution for Cu in the nominal composition $Bi_2Sr_2Ca_2Cu_{3-y}Nb_yO_z$ ($y < 0.3$), as shown in Fig. 3. It is known that the formation of the 2223 phase is not favored when the stoichiometry of Cu is less than 3 in the $Bi_2Sr_2Ca_2Cu_xO_y$ system; however, the 2223 phase can be still obtained as the main phase even if the ratio of Cu in the sample doped with Nb is equal to 2.7, as can be seen from Fig. 3 ($x = 0.3$). This means that Nb replaces Cu in the lattice.
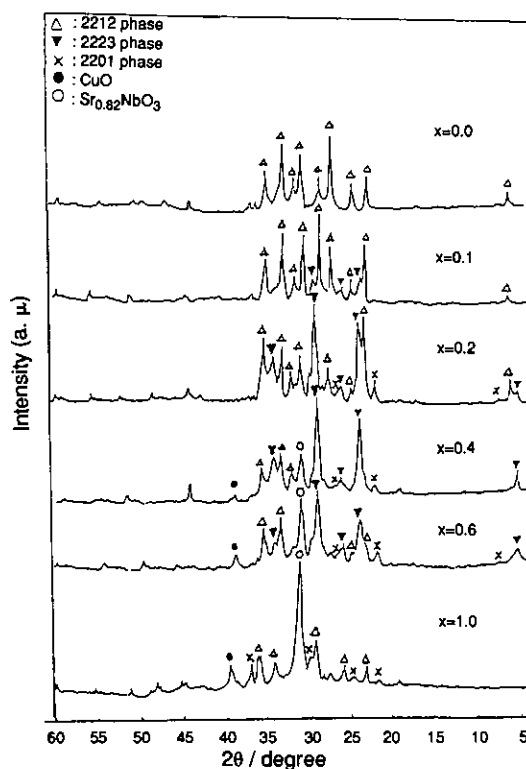
When the sintering temperature is rapidly decreased from 880 to 860°C, these residual phases, together with the 2212 phase, are further reduced; at the same time, the 2223 phase begins to crystallize. If the sample is kept at 860°C for 140 hr, the 2223 high-T_c phase becomes dominant. The following sequence of the transformation mechanism of the three superconducting phases is proposed:

(1) $Bi_2Sr_2CuO_6 + Ca_2CuO_3 + CuO \rightarrow 2Bi_2Sr_2CaCu_2O_8$

(2) $Bi_2Sr_2CaCu_2O_8 + (1/2)Ca_2CuO_3 + (1/2)CuO \rightarrow Bi_2Sr_2Ca_2Cu_3O_{10}$.
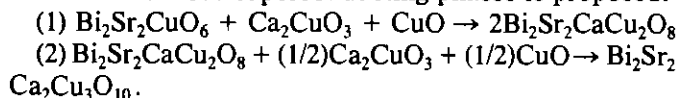
The short-time heat treatment (880°C) and optimal firing temperature (860°C) are vital for accelerating formation of the 2223 phase doped with high-valence cations.

In Fig. 2 we compare the XRD of samples with different levels of Nb doping. With an increase of Nb the amount of the 2212 phase markedly diminishes, and the 2223 phase increases (from $x = 0.0$ to $x = 0.4$). When [Nb] = 0.4, peaks due to the 2212 phase are very weak, and the 2223 phase becomes the main phase. When [Nb] > 0.4, the

FIG. 2. X-ray diffraction patterns of $Bi_{2-x}Nb_xSr_2Ca_2Cu_3O_y$ ($x = 0.0$, 0.1, 0.2, 0.4, 0.6, and 1.0).
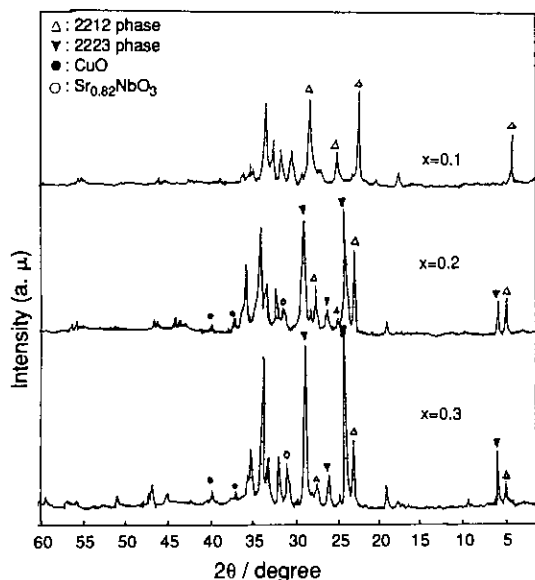
FIG. 3.   XRD of $Bi_2Sr_2Ca_2Cu_{3-x}Nb_xO_y$.

The XRD patterns of samples doped with V or Ta show the same trend as those doped with Nb; the impurity phases associated with peaks at $2\theta = 29° \sim 31°$ are attributed to $Sr_4V_2O_9$ and $Sr_3Ta_2CuO_9$, respectively. These compounds exhibit the same result, where $x = 0.4$ represents the optimum doping amount for all three elements for formation of the 2223 phase. The formation of the 2223 phase proceeds at the fastest rate. Deviation from this optimal composition yields clearly harmful effects. The optimum doping range is so narrow that this may be one of the reasons why these three higher valence cations were not previously found to be as beneficial as Pb.

Generally, doping with these high-valency cations may lead to the lowering of the melting points of samples, but these are still $\sim 10°C$ higher than those of the corresponding Pb-doped samples. The optimum firing temperature

In connection with the probable instability of the 2223 phase, we suggest that the interlayer linkage is weaker in the $Ca-CuO_2-Ca$ layers, as shown in the outlined section of Fig. 4a. The bonding between the Ca layer and the CuO_2 layer becomes weaker when another Ca layer lies on the other side of CuO_2, and the O of the planar CuO_2 layer is not so readily available for coordination as that from a square pyramid, where four basal O are somewhat tilted toward the Ca atom. This leads to a certain degree of instability in the 2223 structure. With substitution of a high-valency cation for the 4-coordinated Cu, more O is incorporated into the lattice and enters the $\otimes$ site, as shown in Fig. 4b (4, 5). The additional M–O interlayer binding is reinforced; thus, the 2223 phase is stabilized.

By analyzing the Bi_{4f} XPS spectra shown in Fig. 5, we deduce that the samples doped with Nb undergo a reversible reaction of $Bi^{5+} + Bi^+ \rightarrow Bi^{3+}$ from quenching to annealing, implying a large change in the Bi–O layer after doping with a high-valency cation. In connection with the O_{1s} spectra in Fig. 6, we believe that the new peak at the lower binding energy (~ 527 eV) in curve a is due to the O_{1s} oxygen bonding with Bi^+ to form Bi^+-O^{2-}. This shows that high-valency cations may substitute not only for Cu but also for Bi. With Nb^{5+} substitution for Bi^{5+}, more bonding oxygens can be absorbed into Bi–O layers, which is beneficial for the formation of the 5-coordinated Aurivillius phase (6), as shown in Fig. 7. Aurivillius structures within the Bi–O layers are favorable for the stability of the 2223 phase (7).
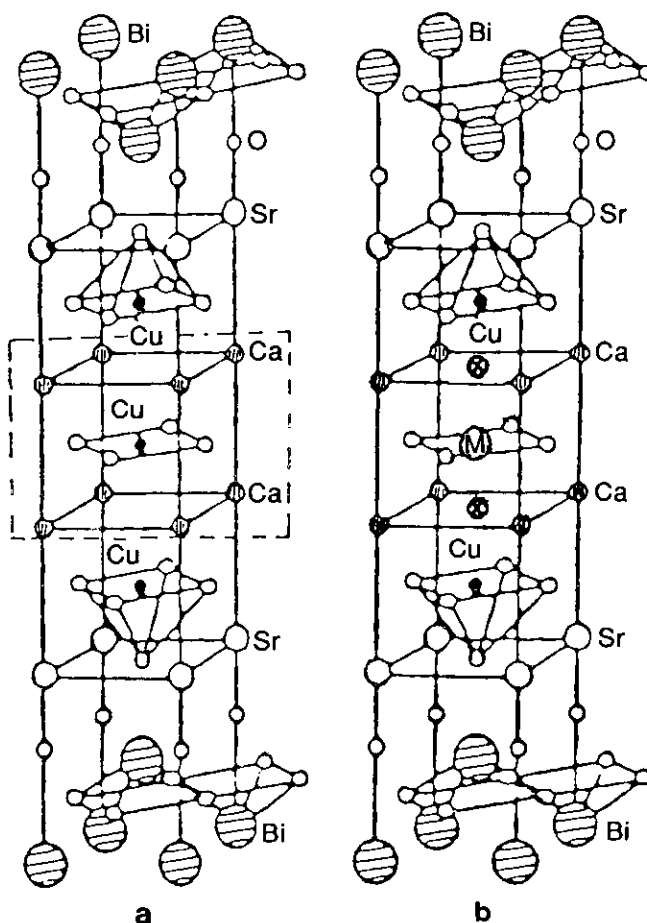

FIG. 4.   Scheme showing the stabilization of the 2223 phase by partial substitution of Cu with a high-valency cation M. (a) Unsubstituted 2223 phase. The outlined section shows the supposed weaker interlayer linkage. (b) Substituted 2223 phase. $\textcircled{M}$ stands for high valency M; $\otimes$ stands for extra 0 added.
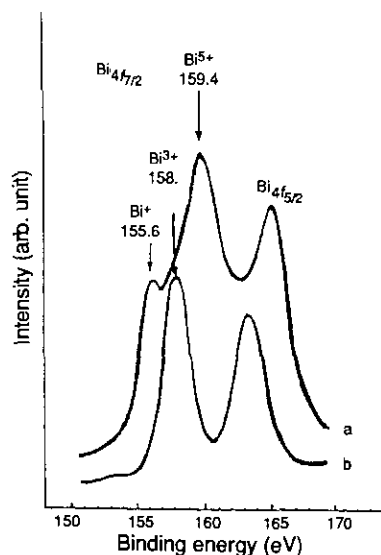
FIG. 5. The core spectra of Bi_{4f} in $Bi_{1.6}Nb_{0.4}Sr_2Ca_2Cu_3O_y$ for (a) air-quenched sample at 860°C, and (b) air-annealed sample at 600°C for 10 hr.
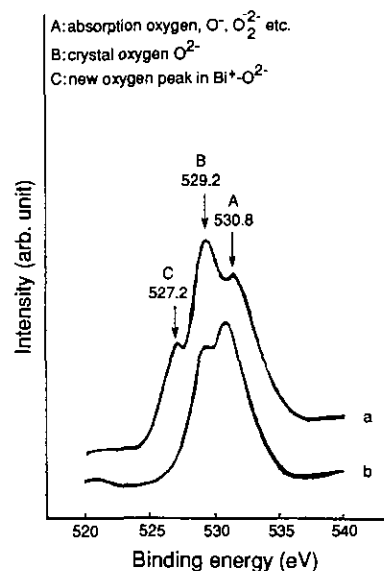
FIG. 6. XPS of O_{1s} in $Bi_{1.6}Nb_{0.4}Sr_2Cu_3O_y$ for (a) air-quenched sample at 860°C, and (b) air-annealed sample at 600°C for 10 hr.

range (less than 10°C) is also narrower than that with Pb doping; this may be another reason why Pb was earlier found to be so beneficial for the formation of the 2223 phase.

Figure 8 shows the $R–T$ curves for samples doped with

V, Nb, or Ta at $X = 0.4$. Together with ac susceptibility measurements it is found that doping with high-valency cations lowers T_c by several degrees near 100 K. There is no amelioration through long-time, low-temperature annealing; only at higher doping levels ($x > 0.4$), with anneal-
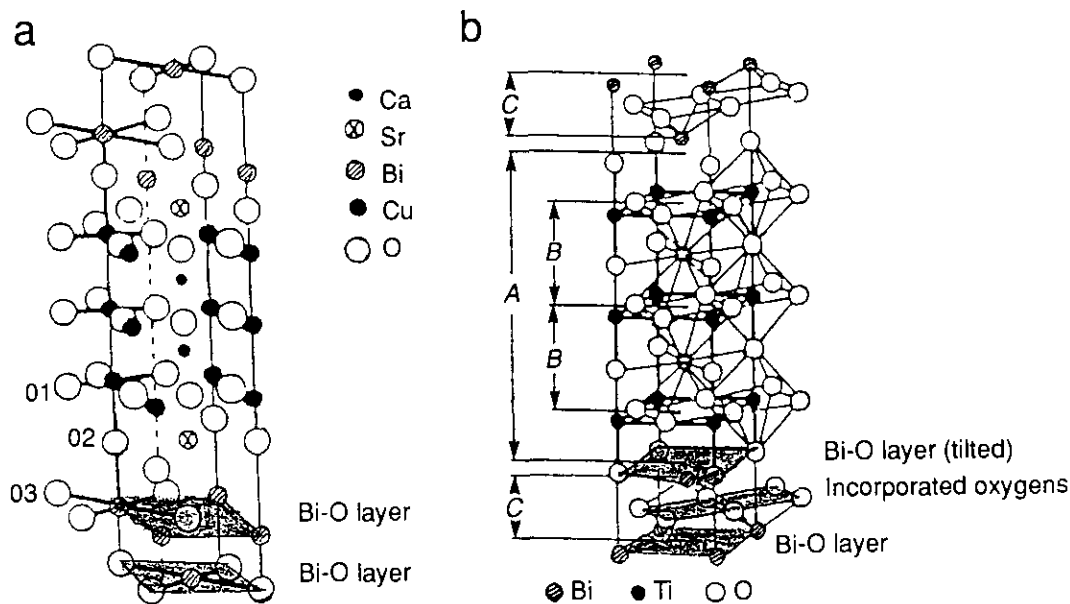

FIG. 7. (a) Schematic illustration of the structure of the $n = 3$ (2223) phase showing the double BiO layers. (b) Schematic illustration of the structure of the Aurivillius phase, which consists of the double BiO layers separated by a layer of oxygen.
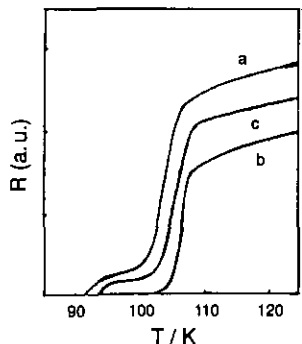
FIG. 8. Temperature dependence of the resistivity for $Bi_{1.6}M_{0.4}Sr_2Ca_2Cu_3O_y$ for (a) $M = V$, (b) $M = Nb$, and (c) $M = Ta$.

ing at 600°C, is the diamagnetism of samples significantly greater than that of the quenched samples, as can be seen from Fig. 9. The may be due to the more random defects distribution in the lattice resulting from incorporation of high-valency cations, especially with regard to change of oxygen voids and number of carriers (8).

The surface morphologies of $Bi_{2-x}Nb_xSr_2Ca_2Cu_3O_y$ ($x = 0.0 \sim 1.0$) samples examined by SEM show clearly a certain degree of alignment of the plate-like grains of the 2223 phase, which is enhanced by increasing the doping level of Nb ($x = 0.0–0.5$), indicating an orientation of the plates along the c-axis. In particular, in the sample with $x = 0.4$, almost all grains are of the plate type and aligned.

After doping with high-valence cations in Bi-based material, some unusual phenomena are observed. Figure 10 shows the Cu_{2p} XPS spectra of $Bi_{1.6}Nb_{0.4}Sr_2Ca_2Cu_3O_y$. It can be clearly seen that the main peak of $Cu_{2p_{3/2}}$ located at about 934.5 eV is higher than that of the 933-eV peak
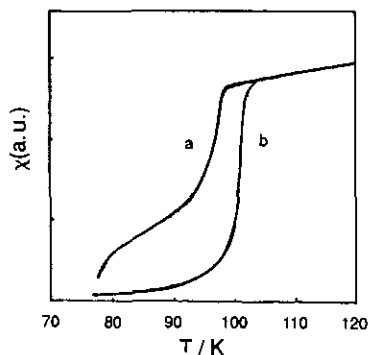
in CuO, indicating the presence of the "Cu^{3+}" oxidation state. From the XPS of the oxides of copper (9, 10), the peak binding energy at 934.5 eV has been assigned to the final state of $3d^9L^{-1}$ and $3d^{10}L^{-2}$, rather than to the $3d^8$ electric configuration, meaning that the above-mentioned Cu^{3+} of the Nb-doped sample exhibits the quasi-high-valence state of Cu.

From the thermogravimetric analysis (TGA) experiment with $Bi_{1.6}Nb_{0.4}Sr_2Ca_2Cu_3O_y$, it is known that incorporation of lattice oxygen at about 630°C is reversible. However, the change of lattice oxygen content is closely related to the density of oxygen vacancies in the crystal structure (11). Thus, the change of the distribution and the amount of oxygen defects are linked to doping with high-valence cations.

The effect of promoting the 2223 phase is also observed in the samples doped with other high-valency cations, for example, in $Bi_{1.9}Sb_{0.1}Sr_2Ca_2Cu_3O_y$, $Bi_{1.6}Mo_{0.4}Sr_2Ca_2Cu_3O_y$, and $Bi_{1.6}Si_{0.4}Sr_2Ca_2Cu_3O_y$.

In summary, doping by V^{5+}, Nb^{5+}, or Ta^{5+} high-valency cations greatly enhances the formation of the 2223 phase, the optimum nominal composition being $Bi_{1.6}M_{0.4}Sr_2Ca_2Cu_3O_y$($M = V$, Nb, or Ta). We argue that the beneficial

FIG. 9. Temperature dependence of ac magnetic susceptibilities χ of $Bi_{1.4}Nb_{0.6}Sr_2Ca_2Cu_3O_y$ (a) quenched in air and (b) postannealed at 600°C for 12 hr.
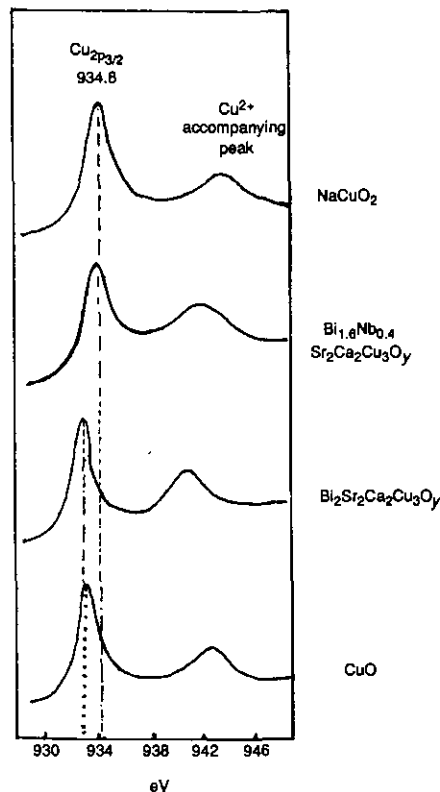

FIG. 10. XPS of Cu_{2p} in samples.

effect of promoting the formation of the 2223 phase might be a general property of doping with high-valency cations.

REFERENCES

1. H. Maeda and Y. Tanaka, *Jpn. J. Appl. Phys.* **27**, 209 (1989).
2. S. A. Sunshine and T. Siegrist, *Phys. Rev. B* **38**, 893 (1988).
3. P. G. Bai and J. Liu, *Chin. J. Acta Phys. Sinica* **40**, 1869 (1991).
4. Y. M. Li, Y. R. Li, *et al.*, *Eur. J. Solid State Inorg. Chem.*, in press.
5. R. K. Li and Z. Y. J. Xu, *J. Solid State Chem.* **94**, 206 (1991).
6. R. Ramesh, M. S. Hegde, *et al.*, *J. Appl. Phys.* **66**, 4878 (1989).
7. F. X. Chen, W. J. Zhu, *et al.*, *Chin. J. Acta Phys. Chem. Sinica* **6**, 519 (1990).
8. Y. R. Li and Y. M. Li, *Chin. J. Acta Phys. Sinica* **42**, 455 (1992).
9. B. Van der Lann, *et al.*, *Phys. Rev. B* **23**, 4369 (1981).
10. N. L. Wang, *et al.*, *Sci. China* **35**, 853 (1992).
11. Yue Wu, *et al.*, *J. Catal.* **120**, 88 (1989).